

AXIALLY EQUILIBRATED DISPLACEMENT-BASED BEAM ELEMENT: IMPLEMENTATION IN OPENSEES AND APPLICATION TO DYNAMIC ANALYSIS OF STRUCTURES

Danilo Tarquini¹, João P. Almeida¹, and Katrin Beyer¹

¹Earthquake Engineering and Structural Dynamics Laboratory (EESD)
École Polytechnique Fédérale de Lausanne (EPFL)
{danilo.tarquini, joao.almeida, katrin.beyer}@epfl.ch

Keywords: OpenSees, Dynamic Analysis, Beam Element, Displacement-based, Axial Equilibrium.

Abstract. *Experimental tests on the inelastic behavior of RC bridge piers have shown that, due to tension shift effects, the curvature profile above the base section of the structural member differs from the one that would develop according to a force-based or a classical displacement-based beam formulation with plane section hypothesis. Due to the inclined cracks in concrete members, it was found that the curvature distribution evolves in a bilinear shape along the member height during the inelastic phase of the response, and that the length of plastification increases with increasing ductility demands.*

Recently, it was shown that axially equilibrated displacement-based elements can more effectively predict the local-level response of RC members. The process of imposing the equilibrium of the axial forces along the element length allows the beam element to improve the simulation of both curvature and strain profiles. The finite element was originally implemented in the authors' structural analysis software SAGRES, which was developed for nonlinear static analysis and is not freely available to the engineering community. This paper presents the validation of the implemented axially equilibrated displacement-based element in the open source finite element software OpenSees and provides some application examples of both nonlinear static and dynamic analyses. The results are compared against classical approaches (force-based and displacement-based), pinpointing the advantages of the axially equilibrated displacement-based beam element.

1 INTRODUCTION

Distributed plasticity Euler-Bernoulli beam element models are a commonly employed simulation tool for the nonlinear analysis of reinforced concrete (RC) structures. Among them, two main approaches are usually distinguished depending on the imposed independent fields: displacement-based (DB) and force-based (FB) formulations. While the former employs linear and Hermitian polynomial functions for the axial and transversal displacement fields, the latter uses constant and linear shape functions for the axial force and bending moment. The advantage of FB elements rely on the fact that the assumed independent fields result in an exact solution regardless of the material nonlinearity. On the other hand, the constraints on the deformation fields imposed by the DB element yield to an exact solution only in case of linear elastic material and nodal loads. Furthermore, equilibrium in FB formulations is verified pointwise along the element length whereas in DB elements the internal forces are in equilibrium with the nodal forces only in an average sense [1].

Although FB element models provide greater theoretical accuracy with respect to the DB counterpart, they typically do not account for tension shift effects in RC structures. The latter are responsible for the linear distribution of plastic curvatures inside the plastic zone of the structural member [2,3] and, as pointed out by Priestley et al. [4], represent the main reason for the mismatch between the response as obtained from a FB element model and experimental results at the local level.

Recently it was shown that a new axially equilibrated displacement-based elements (DB/ae) can be effectively used to address the abovementioned issue [5]. In fact, such finite element (FE) maintains the hypothesis on the linear curvature profile intrinsic to the classical DB formulations while imposing the equilibrium of the axial forces along the element length. The combination of these two aspects allow the beam element to improve the simulation of local-level quantities such as curvature and strains, which add to reliable predictions of global force-displacement responses.

However, the DB/ae was originally implemented in the authors' Matlab-based structural analysis software SAGRES [6], which: (i) is not available to the engineering community; (ii) is not computationally efficient when large structures are considered; and (iii) only allows for nonlinear static analysis. In order to overcome the previous drawbacks, this paper validates the implementation of the DB/ae in the open source finite element software OpenSees [7] and provides application examples both in the nonlinear static and dynamic analysis cases.

The element state determination is recalled in Section 2 together with one validation example. Section 3 presents several nonlinear analyses performed using the DB/ae element within the OpenSees platform. Conclusions are drawn in Section 4.

2 STATE DETERMINATION AND COMPARISON WITH EXISTING FORMULATIONS

A first displacement-based beam element satisfying axial equilibrium was proposed by Izuzudin et al. [8] for the case of nonlinear-elastic problems. The main differences between their formulation and the one proposed by the authors are [5]: (i) the definition of the lateral displacement field (Hermitian vs quartic); (ii) the approach used to derive the element end forces and tangent stiffness matrix; and (iii) the convergence criterion used to establish the attainment of the internal axial equilibrium. A complete description of the element formulation and the mathematical background behind the axially equilibrated displacement-based element can be found in Tarquini et al. [5] and is not included in this paper. Nevertheless, in the following paragraphs the main aspects of the element state determination are discussed; particular focus

is laid on the distinctive aspects with respect to the classical displacement-based approach (DB/c).

Considering a planar problem and a basic reference system for the beam element, the state determination procedure consists of computing the element basic forces \mathbf{p}_{bsc} and tangent stiffness matrix given a set of incremental basic displacements $\Delta\mathbf{u}_{bsc}$. The main steps for both classical and axially equilibrated displacement-based element are depicted and compared in the flowchart of Figure 1.

In a classical DB beam formulation, a linear shape function for the axial displacement field is employed along the element. Hermitian polynomials are used instead for the transverse displacement field which results in a linear curvature profile. When nonlinear material behaviour is considered, such generalized deformations lead to generalized sectional forces—axial force and bending moment—which are not strictly equilibrated along the element length. The application of the principle of virtual work, on the other hand, assures that equilibrium is verified on an average sense.

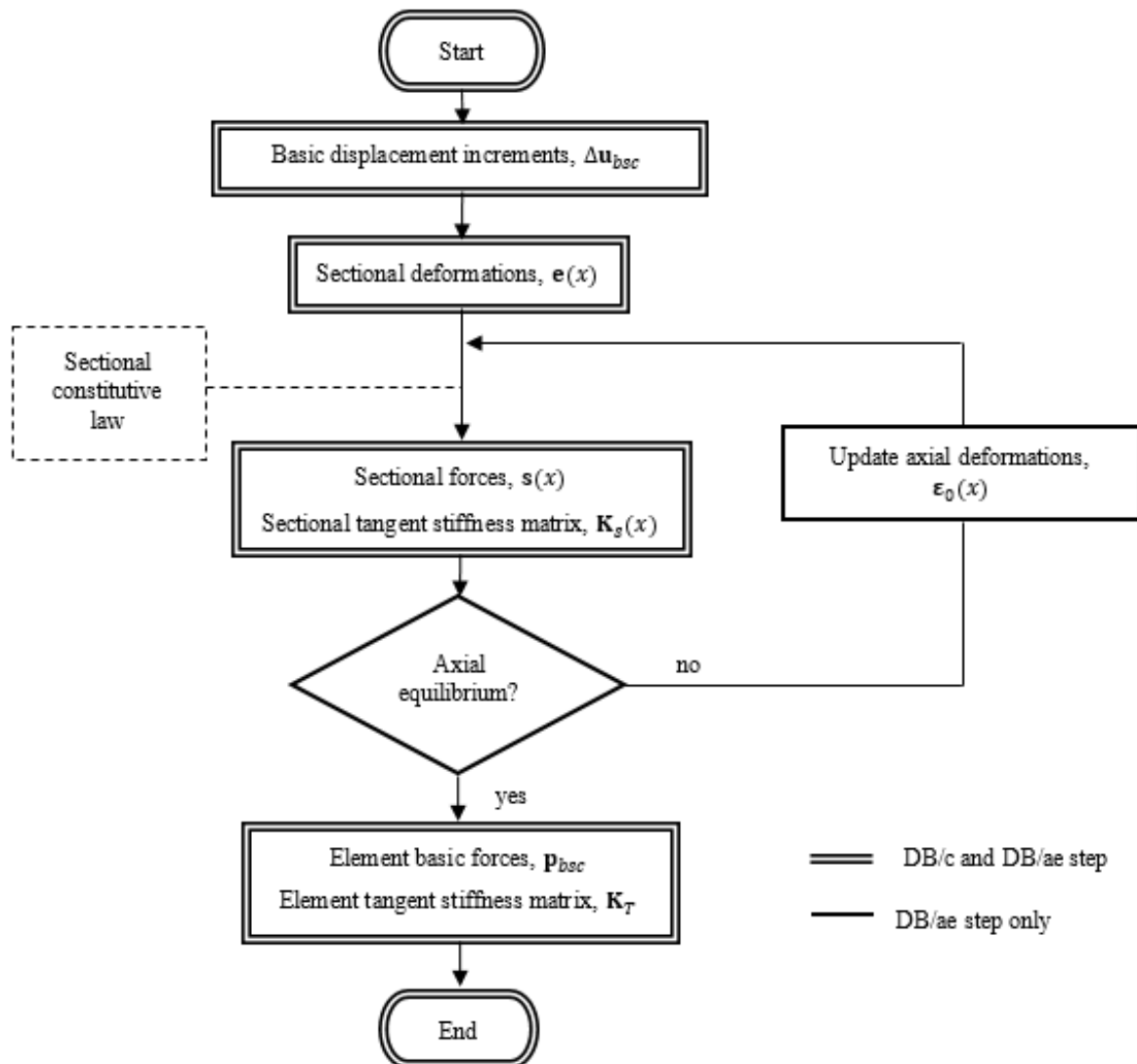


Figure 1: State determination of classical and axially equilibrated displacement-based element (adapted from [5]).

From equilibrium considerations it can be proved that, when only nodal loads are applied, the axial force at all integration sections has to be equal to the basic axial force \mathbf{p}_{bsc}^I . On the other hand, the axial displacement \mathbf{u}_{bsc}^I must be equal to the integral (along the element length) of the axial strains. The latter are updated iteratively in the axially equilibrated DB element to satisfy strict axial equilibrium along the length (see Figure 1). Once convergence is attained, the element basic forces \mathbf{p}_{bsc} , as well as a consistent element tangent basic stiffness matrix \mathbf{K}_T are finally computed via application of the principle of virtual work.

The accuracy of the axially equilibrated displacement-based element (DB/ae) is validated in Tarquini et al. [5] against two sets of RC bridge columns and RC walls. For completeness, and in order to briefly demonstrate the advantages brought about by the use of the proposed formulation, one case study of a RC wall tested by Dazio et al. [9] is discussed in the next paragraphs. The experimental results are compared both in terms of global (force-displacement) and local (curvature profiles) quantities, against numerical results from models employing DB/ae, DB/c and FB elements.

The cantilevered RC wall specimen chosen for the validation is labeled WSH3; it is 2000 mm long and has a shear span of 4520 mm, corresponding to a shear span ratio $L/h=2.26$. Different flexural and confining reinforcement were provided to the web and boundary element region which are detailed in Dazio et al. [9]. A sketch of the RC walls and an example of a finite element (FE) mesh and sectional discretization used in the comparisons are illustrated in Figure 2 while the employed material properties are reported in Table 1. The model proposed by Mander [10] and Menegotto-Pinto [11] were used for concrete and steel respectively. The applied axial load was 686 kN corresponding to an axial load ratio (ALR) of 5.8%.

The beam element models used to simulate the experimental results are briefly described below. Justification and reasoning behind these choices are given in Tarquini et al. [5]. Two models composed of a single FB element are considered, featuring three and five Gauss-Lobatto integration sections. Two models for classical and axially equilibrated displacement-based formulations are also included in the comparison, featuring one and two finite elements per structural member and four Gauss-Lobatto integration sections within each FE. For the cases where the structural member is discretized with two finite elements, the length of the base element is selected as the height of the plastic zone L_{pz} , defined in Dazio et al. [9] as the height at which the plastic curvature profile is equal to the yield curvature

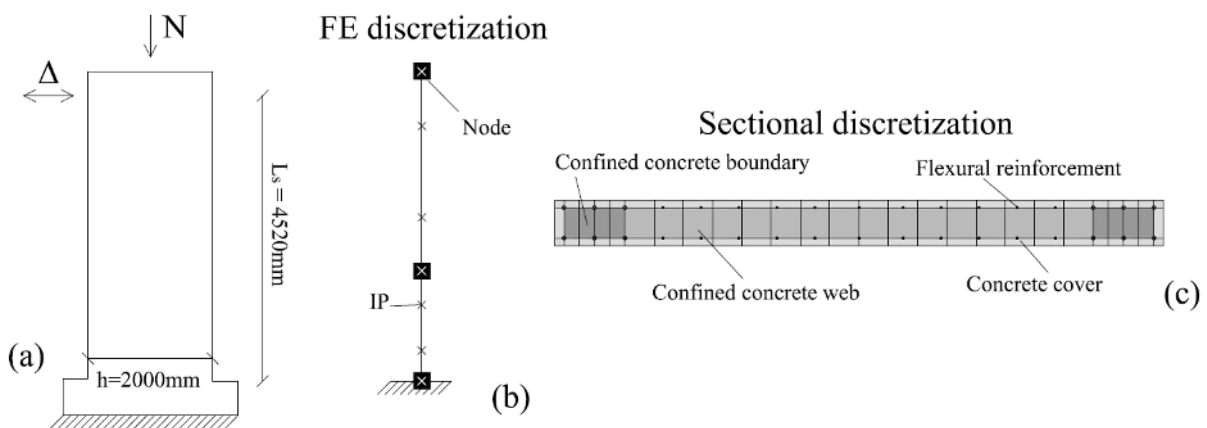


Figure 2: (a) Sketch of specimen WSH3; (b) FE discretization (DB models with two elements per member); (c) Sectional discretization (adapted from [5]).

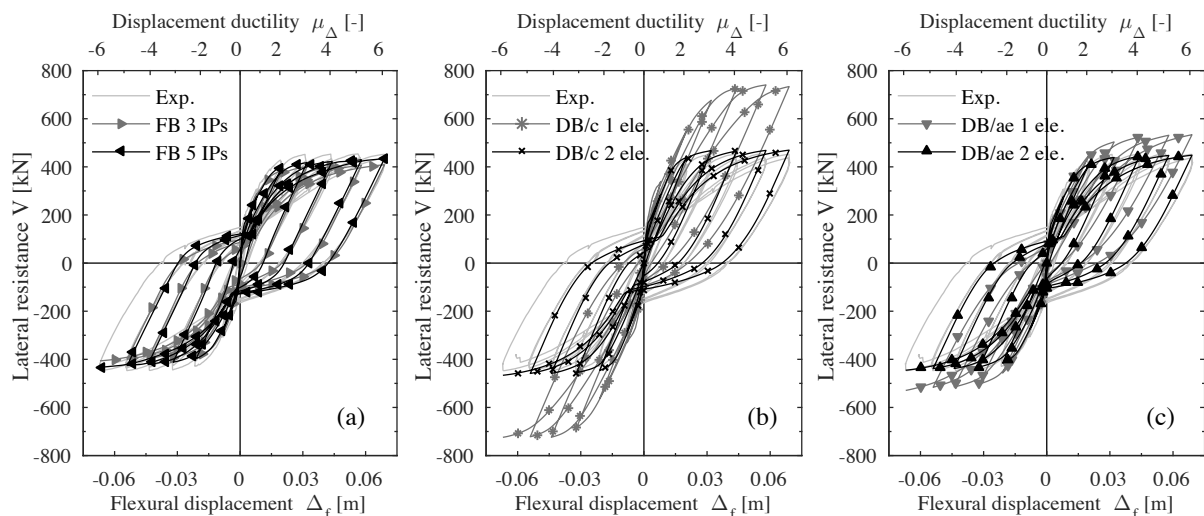
	Concrete					Reinforcing steel				
	f'_c [MPa]	ε_c [‰]	E_c [GPa]	f'_{cc} [MPa]	ε_{cc} [‰]	f_y [MPa]	f_u [MPa]	E_s [GPa]	b [‰]	
Web	39.2	2	35.2	41.8	2.7	Ø8 mm	570	700	200	9.3
Boundary	39.2	2	35.2	48.1	4.2	Ø12 mm	601	725	200	8.4

Table 1: Steel and concrete material properties.

The experimental and numerical force-displacement responses for all the models discussed above are compared in Figure 3. Flexural displacements (computed by subtracting the displacement due to shear and base rotation from the total displacement) are reported on the bottom x -axis. The displacement ductility referred to the total lateral displacement is instead displayed on the top x -axis. It can be observed that models using one FB element or two DB elements (both DB/c and DB/ae) predict reasonably well the structural response. Among the FB element models, the model with five IPs yields the best simulation as the model with three IPs slightly underestimates the experimental results. Both DB models using a single element overestimate the experimental hysteretic curve, although the error associated to the DB/ae formulation is sensibly lower than the one given by the DB/c.

As mentioned in the introduction, the main advantage of using the DB/ae formulation lies in the possibility of capturing tension shift effects occurring in RC members. This allows for more accurate simulations of local-level quantities when compared to classical approaches. Figure 4 illustrates the above considerations by contrasting experimental and numerical curvature profiles for different levels of displacement ductility. Models using one FB with five IPs and two DB elements per member (using both classical and axially-equilibrated formulations) are used. Observations on the performance of the different models are summarized next: (a) The FB model tends to overestimate the actual curvature profiles, especially for large drift levels; (b) The opposite trend is depicted by the DB/c model, which underestimates the actual curvature profile. Moreover, when such elements are employed, the numerical curvature profiles are discontinuous between elements, which results from the average (i.e., non-strict) equilibrium verification along each finite element; (c) The match between observed and calculated curvature profiles is largely improved if DB/ae are used.

Similarly, vertical strain profiles are also better simulated by DB/ae with respect to FB and DB/c. The comparison of these vertical strain profiles is carried out in Tarquini et al. [5].


 Figure 3: Experimental *versus* numerical F- Δ response: (a) FB models; (b) Classical DB models; (c) Axially equilibrated DB models (analysis performed for document [5]).

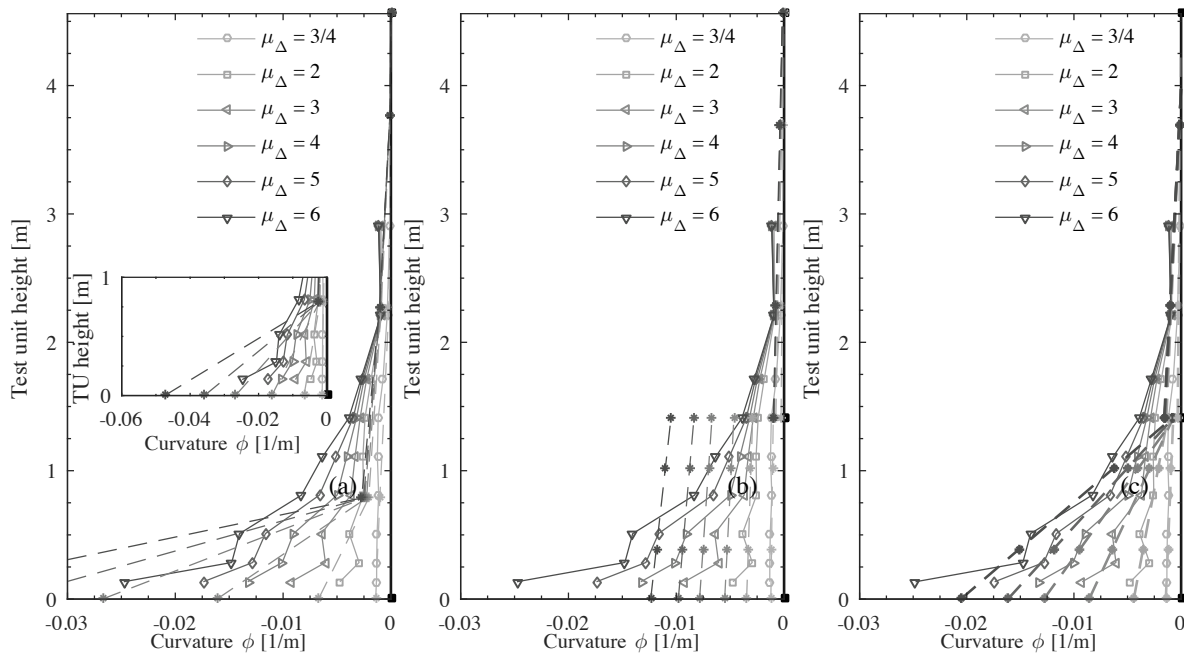


Figure 4: Experimental *versus* numerical curvature profiles: (a) Force-based; (b) Classical displacement-based; (c) Axially equilibrated displacement-based (analysis performed for document [5]).

3 IMPLEMENTATION IN THE SOFTWARE OPENSEES

The axially equilibrated displacement-based element was implemented in the open source software OpenSees [7]. At present it is available as an external software library and it will be provided upon request to the authors of this paper. The authors will also formally ask the finite element to be integrated in the core of OpenSees.

The DB/ae element presents no difference in use with respect to other available nonlinear beam column elements for 2D (planar frame) analysis. The label required to call it within the software environment is ‘dispBeamColumnAxEq’¹. The input parameters to be defined are the same required for the ‘dispBeamColumn’ element (i.e., OpenSees label used to call classical DB element) except for the fact that the tolerance limit must be additionally explicitly defined. The latter expresses the maximum axial force unbalance accepted between different integration sections. Appropriate documentation and verification examples will be provided by the authors together with the external library containing the element implementation until the DB/ae will be officially included in the software core. An appropriate documentation will be added to the software user’s manual and within the several online documentation websites.

In the following two subsections results from several models employing DB/ae elements are illustrated and discussed, both in the framework of nonlinear static and dynamic analysis. OpenSees models are also compared to the corresponding SAGRES [6] models with a two-fold objective: on the one side to validate the FE implementation and on the other to compare the computational time.

3.1 Nonlinear Static analysis

A simple case study corresponding to a virtual 3 m cantilever column—Figure 5(a)—is used to validate the implementation of the DB/ae in OpenSees. The square 200x200 mm RC section is composed by 20 concrete fibers (discretized only in the bending direction) and 12

¹ It may vary once the element is officially released. Always refer to the OpenSees online guide: <http://opensees.berkeley.edu/wiki/index.php>

steel fibers representing 10 mm-diameter rebars. The OpenSees material models [12] Concrete04 and Steel02 are employed for concrete and steel fibers respectively. The main material parameters are listed in Table 2. A single finite element with four Gauss-Lobatto integration sections is used to discretize the structural member.

Figure 5(b) displays the results of three pushover analysis for three values of axial load ratios (ALR): 1%, 5%, and 10%. DB/ae elements are used in all three cases. The label OS (OpenSees) and SA (SAGRES) stand for the software used to perform the simulation. As expected, the force capacity increases with the imposed ALR while the perfect superposition between the curves for the same ALR confirms the good implementation of the DB/ae element in OpenSees.

Nonlinear cyclic static analyses from three models involving a single FB, DB/c and DB/ae element are compared in Figure 5(c). The strongest and stiffest response is unsurprisingly provided by the DB/c element model due to the constraints imposed in both the axial and transversal displacement fields. By imposing axial equilibrium, and thus removing the axial strain constraint, the model using one DB/ae element shows a reduction in the simulated lateral strength. However, the latter is still larger than the solution provided by the FB formulation, where no displacement fields are assigned and exact equilibrium is satisfied. Again, the fact that no difference can be seen between results from the same model but originating from different software confirms that the DB/ae is correctly implemented.

Computational time for both pushover and cyclic analyses, using the same central processing unit, are displayed in Table 3 showing that: (i) The performance of the DB/ae is similar to both DB/c and FB models; and (ii) The OpenSees model runs much faster than the same model in SAGRES, which is a consequence of the different programming language in which the two software were developed (C++ versus Matlab).

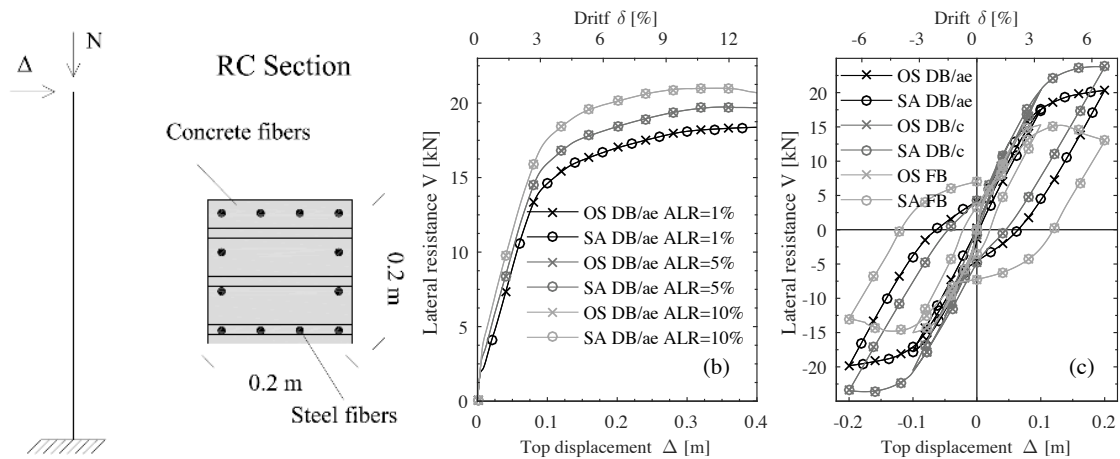


Figure 5: (a) Sketch of the structure and sectional discretization; Comparison between OpenSees and Sagres Models: (b) Pushover analysis for different ALR; (c) Cyclic analysis.

Concrete			Reinforcing steel		
f'_c [MPa]	ϵ_c [‰]	E_c [GPa]	f_y [MPa]	E_s [GPa]	b [‰]
40	2	30	500	200	5

Table 2: Steel and concrete material parameters used in the OpenSees models for static analysis.

Model	Static		Dynamic
	Monotonic	Cyclic	
	T[s]	T[s]	T[s]
SA DB/ae	37	212	[-]
OS DB/ae	2	21	290
OS DB/c	2	18	330
OS FB	2	20	260

Table 3: Computational time for different models and analysis.

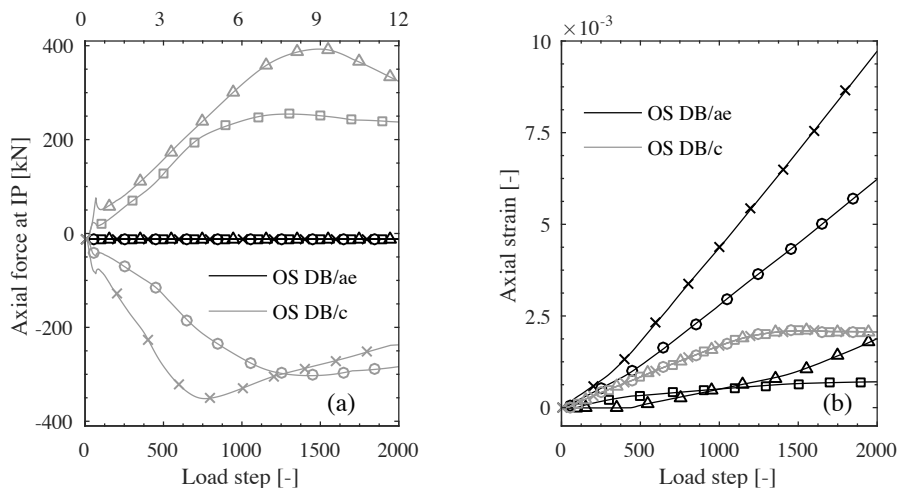


Figure 6: Axial force (a) and axial strain (b) evolution at all IPs for DB/ae and DB/c element models during pushover analysis with OpenSees, ALR 1%.

The sectional axial forces and average axial strains at all IPs were recorded during the pushover analysis (1% ALR) for both the DB/ae and DB/c element model implemented in OpenSees; they are depicted in Figure 6:(a) and Figure 6:(b). For the DB/c case the axial forces are different in the four IPs and equal only in average to the applied axial load (12 kN). On the other hand, for the DB/ae element model the axial force is constant during the analysis in all IPs and equal to the applied external axial load. The opposite behaviour is instead observed for the generalized axial strains: they are the same in all IPs for the DB/c (the axial displacement field is constrained to be linear) while they assume different values for the DB/ae.

3.2 Nonlinear time history analysis

One advantage of implementing the DB/ae formulation in OpenSees is that it can be used for nonlinear time history simulations as well. Such analysis type is not available in SAGRES, which currently features only the nonlinear static analysis solver [6]. A RC column tested at the UCSD's Englekirk Structural Engineering Center in occasion of the 'Concrete Column Blind Prediction Contest 2010' [13] is used as case study. The finite element models selected to carry out the analysis discretize the structural member with a single FB, two DB/c and two DB/ae elements. The height of the bottom one is taken as twice the plastic hinge length computed according to the formula proposed by Priestley et al. [4]. This length was deemed to be a good estimate of the maximum height over which the plastic curvature profile intersects the elastic one [5]. Each FE has four integration sections; different fibers are used to model

cover concrete, core concrete and longitudinal reinforcing bars. The material models and respective main parameters are summarized in Table 4. A zero-length element is employed to simulate the strain penetration of the flexural reinforcement into the footing, as suggested by Zhao and Sritharan [14]. Tangent stiffness proportional damping (1% at the first vibration mode) is assumed and nonlinear geometrical effects are considered through the use of the co-rotational formulation.

Concrete (Concrete04)					Reinforcing steel (Steel02)		
f'_c [MPa]	ϵ_c [‰]	E_c [GPa]	f'_{cc} [MPa]	ϵ_c [‰]	f_y [MPa]	E_s [GPa]	b [‰]
41.5	2.8	30	50	5.5	518	200	8

Table 4: Steel and concrete material models and parameters used in OpenSees for dynamic analysis.

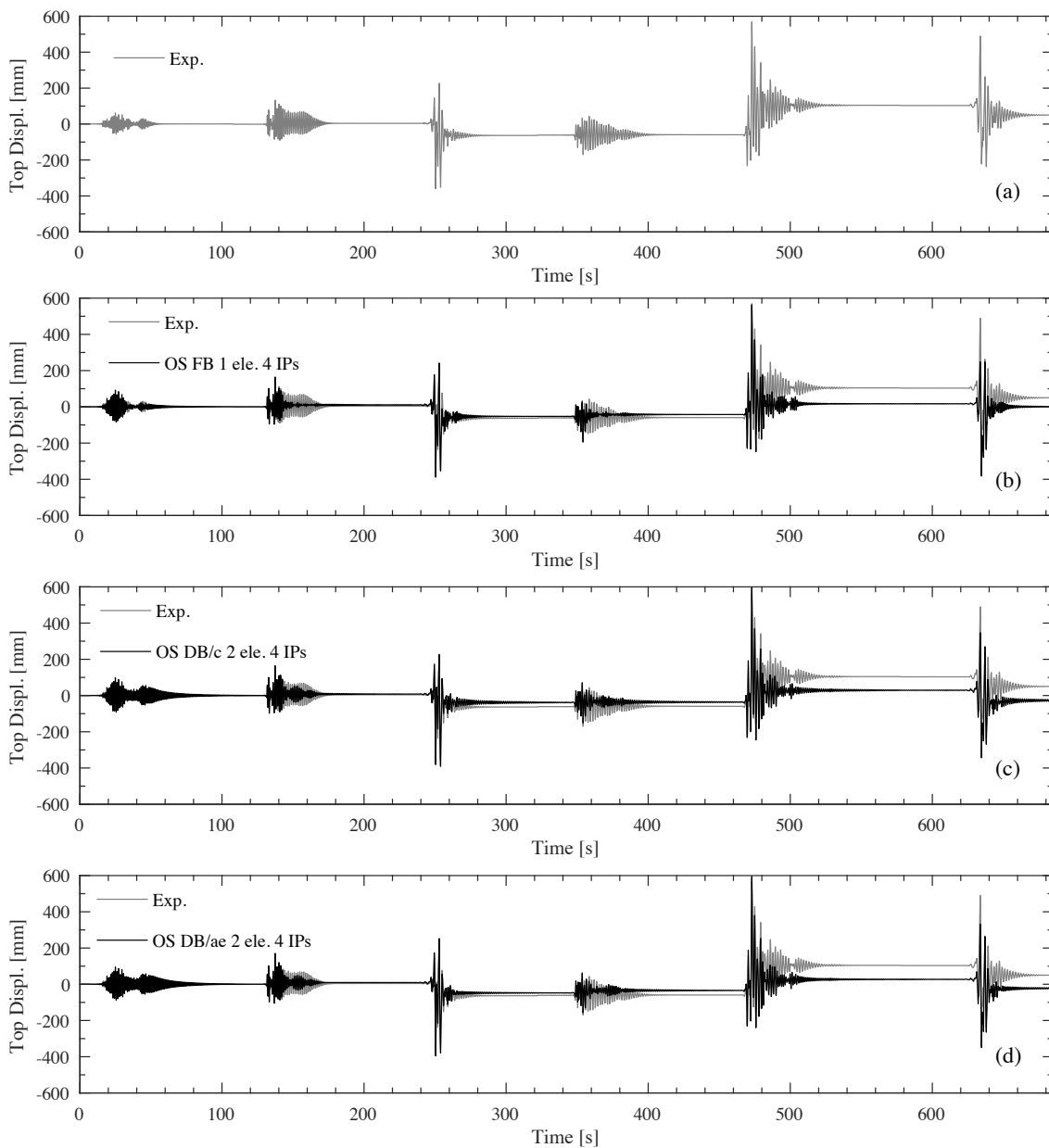


Figure 7: (a) Experimental top displacement time histories; Numerical *versus* experimental top displacement time histories: (b) FB; (c) DB/c; (d) DB/ae.

The numerical *versus* experimental top displacement histories are illustrated in Figure 7; in order to ease the comparison the experimental results are displayed alone in Figure 7(a). It can be observed that the numerical response is similar for all the considered FE models and that the match with the experimental results is reasonably good, at least up to the pulse of the fourth ground motion. After this point there is a residual displacement which is not captured by any of the considered models which causes the offset between numerical and experimental results. Finally, from the computational time viewpoint, the DB/ae model analysis (which consists of around 170000 time steps) takes around 5 minutes to run in a regular office PC, which is similar to the computing time when DB/c or FB elements were used (see Table 3).

4 CONCLUSIONS

The present paper shows the implementation validation and use of a newly developed axially equilibrated displacement-based element in the open source software OpenSees. The element has been shown to yield good predictions of global and local response parameters of RC members. Currently it is available as an external OpenSees library but it will be submitted to be included in the software core.

The beam element was tested numerically under different load conditions and analysis types. Namely, it was verified under nonlinear static (monotonic and cyclic) and dynamic analysis, showing in all cases a similar performance in terms of computational time with respect to the one provided by classical force-based or displacement-based formulations.

REFERENCES

- [1] A. Calabrese, J.P. Almeida, R. Pinho, Numerical issues in distributed inelasticity modeling of RC frame elements for seismic analysis, *J. Earthq. Eng.* 14 (2010) 38–68. doi:10.1080/13632469.2010.495681.
- [2] E.M. Hines, J.I. Restrepo, F. Seible, Force-displacement characterization of well-confined bridge piers, *ACI Struct. J.* 101 (2004) 537–548.
- [3] J.C. Goodnight, M.J. Kowalsky, J.M. Nau, Modified Plastic-Hinge Method for Circular RC Bridge Columns, *J. Struct. Eng.* (2016). doi:10.1061/(ASCE)ST.1943-541X.0001570.
- [4] M.J.N. Priestley, G.M. Calvi, M.J. Kowalsky, *Displacement-based seismic design of structures*, IUSS Press, 2007.
- [5] D. Tarquini, J.P. Almeida, K. Beyer, Axially equilibrated displacement-based beam element for simulating the cyclic inelastic behaviour of RC members, *Earthq. Eng. Struct. Dyn.* (2017). doi:10.1002/eqe.2865.
- [6] J.P. Almeida, D. Tarquini, SAGRES: Software for Analysis of GRadiant Effects in Structures., *Progr. Dev. Matlab.* (2016).
- [7] F. McKenna, G.L. Fenves, M.H. Scott, B. Jeremic, *Open System for Earthquake Engineering Simulation (OpenSees)*, Berkeley, California, U.S.A., 2000.
- [8] B. Izzuddin, C. Karayannis, A. Elnashai, Advanced nonlinear formulation for reinforced concrete beam-columns, *J. Struct. Eng.* 120 (1994) 2913–2934.

- [9] A. Dazio, K. Beyer, H. Bachmann, Quasi-static cyclic tests and plastic hinge analysis of RC structural walls, *Eng. Struct.* 31 (2009) 1556–1571.
<http://www.sciencedirect.com/science/article/pii/S0141029609000698> (accessed November 16, 2013).
- [10] J.B. Mander, M.J.N. Priestley, R. Park, Theoretical Stress-Strain Model for Confined Concrete, *J. Struct. Eng.* 114 (1988) 1804–1826.
- [11] M. Menegotto, P.E. Pinto, Method of analysis for cyclically loaded RC plane frames including changes in geometry and non-elastic behaviour of elements under combined normal force and bending., in: *IABSE Symp. Resist. Ultim. Deform. Struct. Acted by Well Defin. Repeated Loads - Final Rep.*, 1973.
- [12] S. Mazzoni, F. McKenna, M.H. Scott, G.L. Fenves, *OpenSees command language manual*, (2006).
- [13] NEES@UCSD, *Concrete Column Blind Prediction Contest*, (2010).
<https://nees.org/warehouse/experiment/2838/project/987>.
- [14] J. Zhao, S. Sritharan, Modeling of strain penetration effects in fiber-based analysis of reinforced concrete structures, *ACI Struct. J.* 104 (2007) 133–141.